Cutter head spillage when dredging sand or gravel

Miedema, Sape; Nieuwboer, Bas

Publication date
2019

Document Version
Final published version

Published in
Proceedings of the Dredging Summit and Expo 2019

CUTTER HEAD SPILLAGE WHEN DREDGING SAND OR GRAVEL

Sape A. Miedema[1] & Bas J. Nieuwboer[2]

ABSTRACT

One of the main types of equipment is the cutter suction dredge (CSD). The theoretical soil production Qc equals the cross section of the cutter head in the bank cutting, perpendicular to the swing velocity vs times the swing velocity vs. If the theoretical soil production is 100%, usually less than 100% will enter the suction pipe. The real production. The difference between the theoretical production and the real production is the spillage. So, this is the percentage of the theoretical production not entering the suction pipe.

Now in practice it is more difficult to define the spillage, because often a number of swings at different levels is necessary to excavate a bank. The spillage of a previous swing may be cut a second time during the current swing and thus enter the suction pipe in the current swing. So, the spillage of one swing does not have to be spillage overall. In this report however just one swing is considered, assuming a fresh bank, where all the soil that does not enter the suction pipe is considered spillage.

The model is derived based on the Euler equation for centrifugal pumps, including inner and outer radii and blade angles. The model is first calibrated based on the limited experimental data mentioned in den Burger (2003). This paper covers the theory and the validation, with many experimental data of Miltenburg (1983), a cold case never published before. This paper shows the state of the art of the spillage modeling.

Keywords: Dredging, Spillage, Cutterhead, Cutting Sand & Gravel, Production.

INTRODUCTION

In dredging soils is excavated with dredging equipment. One of the main types of equipment is the cutter suction dredge (CSD). Figure 1 shows a large CSD, the Mashour, build in the 90's for the Suez Canal Port Authorities for maintenance of the Suez Canal. The CSD consists of a floating pontoon, with in the back a spud pole penetrating the soil. In the front there is a ladder, which can rotate around a horizontal bearing. By means of this rotation the cutter head, mounted at the end of the ladder, can be positioned in the soil (the bank). Also, at the end of the ladder two swing wires are connected (port and starboard wires) enabling the CSD to rotate around the spud pole and thus letting the cutter head make a circular movement through the bank. During this rotation, with a circumferential swing velocity $\mathbf{v_s}$ at the center of the cutter head, the cutter head (also rotating around its axis with a certain rpm) is excavating (cutting) the soil. The theoretical soil production $\mathbf{Q_c}$ equals the cross section of the cutter head in the bank cutting, perpendicular to the swing velocity $\mathbf{v_s}$ times the swing velocity $\mathbf{v_s}$. The cutter head consists of the cutter axis connected to the hub (top of the cutter head), 5 or 6 arms on one side connected to the hub and on the other side connected to the ring and a suction pipe to catch the soil cut and transport the soil to its destination. This is shown in Figure 2. If the theoretical soil production is 100%, usually less than 100% will enter the suction pipe. The real production. The difference between the theoretical production and the real production is the spillage. So, this is the percentage of the theoretical production not entering the suction pipe.

Now in practice it is more difficult to define the spillage, because often a number of swings at different levels is necessary to excavate a bank. The spillage of a previous swing may be cut a second time during the current swing and thus enter the suction pipe in the current swing. So, the spillage of one swing does not have to be spillage overall. In this report however just one swing is considered, assuming a fresh bank, where all the soil that does not enter the suction pipe is considered spillage.

A model is derived based on the Euler equation for centrifugal pumps, including inner and outer radii and blade angles. The model is calibrated based on the experimental data mentioned in den Burger (2003). The model gives

[1] Associate Professor, Delft University of Technology, Mekelweg 2, 2628CD Delft, The Netherlands, T: +31-15-2788359, Email: s.a.miedema@tudelft.nl.

[2] PhD, Delft University of Technology, Mekelweg 2, 2628 CD, Delft, The Netherlands, T: ++31-15-2789296, Email: b.j.nieuwboer@tudelft.nl.

almost exactly the same production/spillage curves. Using different radii and blade angles will give a slightly different production curve. Miedema (2018) and Werkhoven et al. (2018), (2019A) and (2019B) published a first and second version of the analytical spillage model. Here the state of the art of the spillage modeling is given.

The ratio of the rotating mixture flow to the mixture flow through the suction mouth must be constant and is used in many graphs as a dimensionless number on the horizontal axis, the Burger number.

$$Bu = \frac{\omega \cdot r_r^3}{Q_m} = constant \quad (1)$$

Figure 1: The Mashour (Suez Canal Port Authorities).

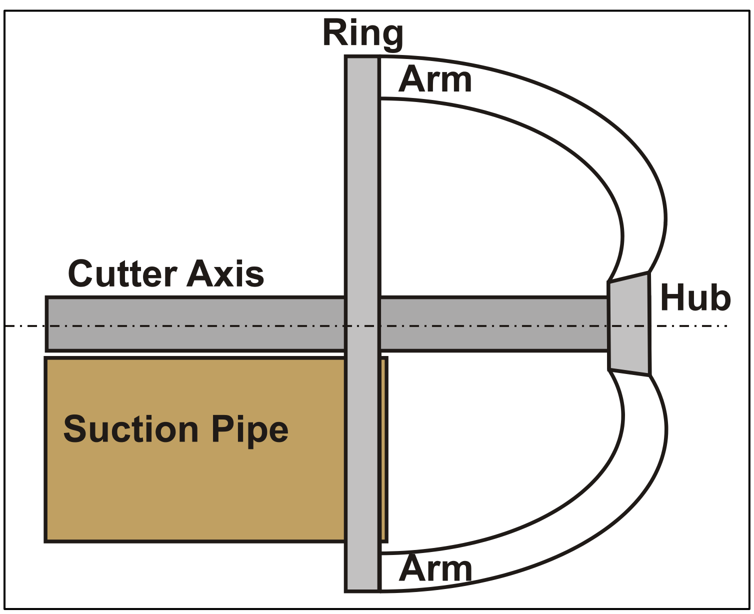

Figure 2: The simplified cutter head.

THE EULER EQUATION

The model starts with the so-called Euler equation. The derivation of this equation can be found in every good text book on centrifugal pumps. The basic Euler equation for centrifugal pumps yields (see Figure 3 for definitions):

$$\Delta p_E = \rho_m \cdot u_o \cdot \left(u_o - \frac{Q \cdot cot(\beta_o)}{2 \cdot \pi \cdot r_o \cdot w} \right) - \rho_m \cdot u_i \cdot \left(u_i - \frac{Q \cdot cot(\beta_i)}{2 \cdot \pi \cdot r_i \cdot w} \right) \tag{2}$$

In terms of radial frequency (like rpm) and radii this gives:

$$\Delta p_E = \rho_m \cdot \omega^2 \cdot \left(r_o^2 - r_i^2 \right) - \frac{\rho_m \cdot \omega \cdot Q}{2 \cdot \pi \cdot w} \cdot \left(cot\left(\beta_o\right) - cot\left(\beta_i\right) \right) \tag{3}$$

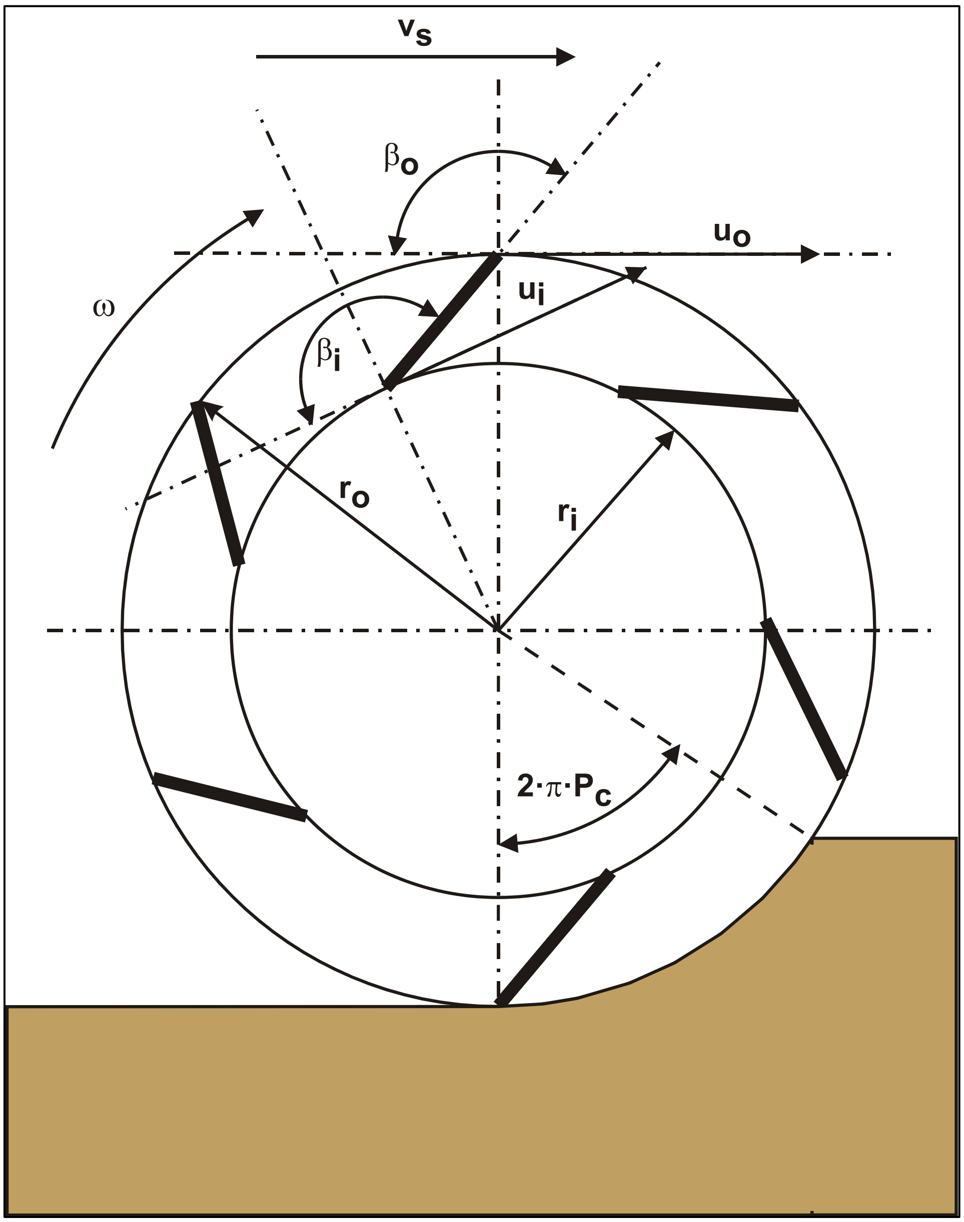

Figure 3: The definitions of the Euler equation for a cutter head.

The flow through the impeller blades can be considered to be, assuming the radial velocity is proportional to the tangential velocity with a proportionality constant α:

$$Q = \alpha \cdot 2 \cdot \pi \cdot \omega \cdot r_o^2 \cdot w \tag{4}$$

The factor α is a constant that can still be anything. Substituting equation (4) in equation (3) gives:

$$\Delta p_E = \rho_m \cdot \omega^2 \cdot \left(r_o^2 - r_i^2\right) - \alpha \cdot \rho_m \cdot \omega^2 \cdot r_o^2 \cdot \left(\cot\left(\beta_o\right) - \cot\left(\beta_i\right)\right) \tag{5}$$

This can be simplified to:

$$\Delta p_E = \rho_m \cdot \omega^2 \cdot \left(\left(r_o^2 - r_i^2\right) - \alpha \cdot r_o^2 \cdot \left(\cot\left(\beta_o\right) - \cot\left(\beta_i\right)\right)\right) \tag{6}$$

THE CUTTER HEAD

The cutter head is assumed to consist of two segments, see Figure 6. Segment 1, near the ring of the cutter head, where mixture flows out of the cutter head and segment 2, near the top of the cutter head, where water flows in to the cutter head and where also axial flow flows into the cutter head, see Figure 7. It is also assumed that for both segments a percentage of the circumference is cutting sand or rock, so this percentage $\mathbf{P_c}$ does not participate in the circular flow causing the spillage. Here this percentage is different for the two segments, which is the case in reality.

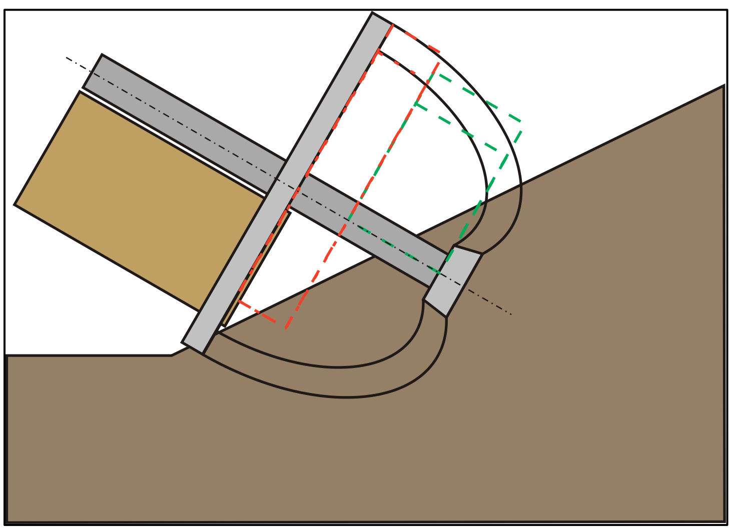

Figure 4: The cutter head in the bank.

The pressure generated by segment 1, the driving pressure is now, assuming mixture flow:

$$\Delta p_{E,1} = \rho_{m,1} \cdot \omega^2 \cdot \left(\left(r_{o,1}^2 - r_{i,1}^2\right) - \alpha_1 \cdot r_{o,1}^2 \cdot \left(\cot\left(\beta_{o,1}\right) - \cot\left(\beta_{i,1}\right)\right)\right) \tag{7}$$

The outflow through segment 1 is (see Figure 7):

$$Q_{1,out} = \alpha_1 \cdot 2 \cdot \pi \cdot \omega \cdot r_{o,1}^2 \cdot w_1 \cdot \left(1 - P_{c,1}\right) \tag{8}$$

The pressure generated by segment 2 is now, assuming another mixture density (see Figure 6):

$$\Delta p_{E,2} = \rho_{m,2} \cdot \omega^2 \cdot \left(\left(r_{o,2}^2 - r_{i,2}^2\right) - \alpha_2 \cdot r_{o,2}^2 \cdot \left(\cot\left(\beta_{o,2}\right) - \cot\left(\beta_{i,2}\right)\right)\right) \tag{9}$$

The outflow through segment 2 without outside pressure from segment 1 is (see Figure 7):

$$Q_{2,out} = \alpha_2 \cdot 2 \cdot \pi \cdot \omega \cdot r_{o,2}^2 \cdot w_2 \cdot \left(1 - P_{c,2}\right) \tag{10}$$

Now suppose the inflow in segment 2 equals the specific flow of segment 1 minus the specific flow of segment 2 times the width of segment 2, this gives (see Figure 7) and corrected for the part of the circumference cutting the soil:

$$Q_{2,in} = \left(\alpha_1 \cdot 2 \cdot \pi \cdot \omega \cdot r_{o,1}^2 - \alpha_2 \cdot 2 \cdot \pi \cdot \omega \cdot r_{o,2}^2\right) \cdot w_2 \cdot \left(1 - P_{c,2}\right) \tag{11}$$

If it is also assumed that the inflow in segment 2 is proportional to the pressure difference between segments 1 and 2, this also gives:

$$\begin{aligned} Q_{2,in} &= \varepsilon \cdot \left(\Delta p_{E,1} - \Delta p_{E,2}\right) \cdot \frac{w_2}{\rho_{m,2} \cdot \omega} \cdot \left(1 - P_{c,2}\right) \\ &= \varepsilon \cdot \omega \cdot w_2 \begin{pmatrix} \dfrac{\rho_{m,1}}{\rho_{m,2}} \cdot \left(\left(r_{o,1}^2 - r_{i,1}^2\right) - \alpha_1 \cdot r_{o,1}^2 \cdot \left(\cot\left(\beta_{o,1}\right) - \cot\left(\beta_{i,1}\right)\right)\right) \\ -\left(\left(r_{o,2}^2 - r_{i,2}^2\right) - \alpha_2 \cdot r_{o,2}^2 \cdot \left(\cot\left(\beta_{o,2}\right) - \cot\left(\beta_{i,2}\right)\right)\right) \end{pmatrix} \cdot \left(1 - P_{c,2}\right) \end{aligned} \tag{12}$$

Since these equations still contain proportionality constants, the main issue is, are the assumptions valid. The assumptions are valid if the spillage found shows the same qualitative behavior, the same shape of spillage or production curves as has been found with experiments.

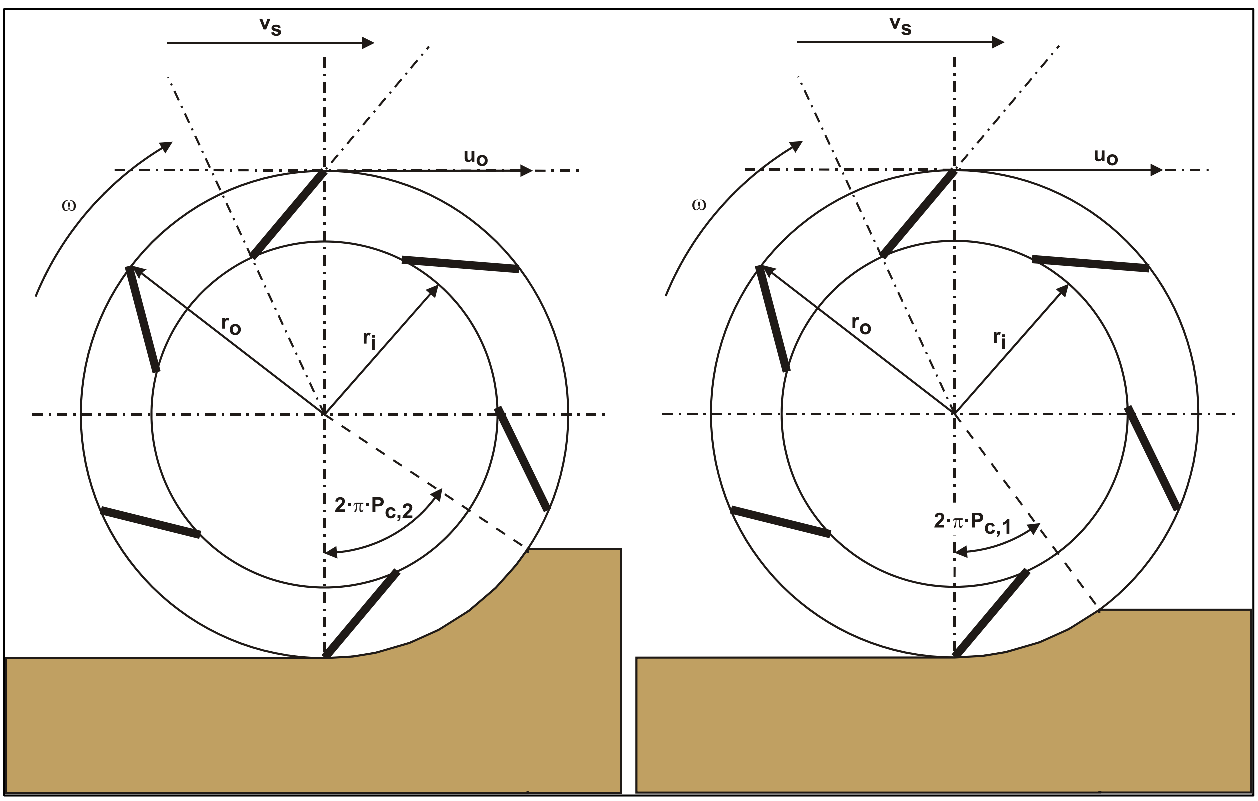

Figure 5: The percentages cut in segments 1 and 2.

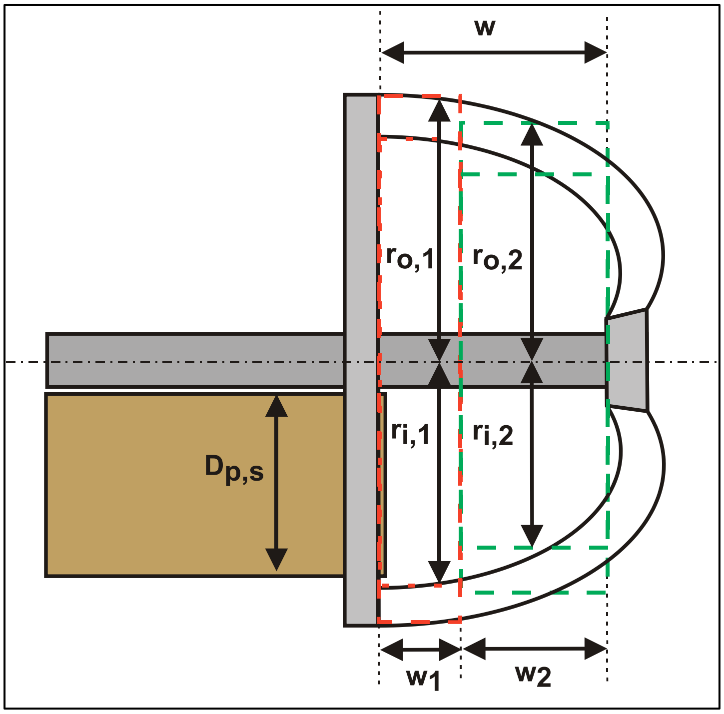

Figure 6: The dimensions of the cutter head.

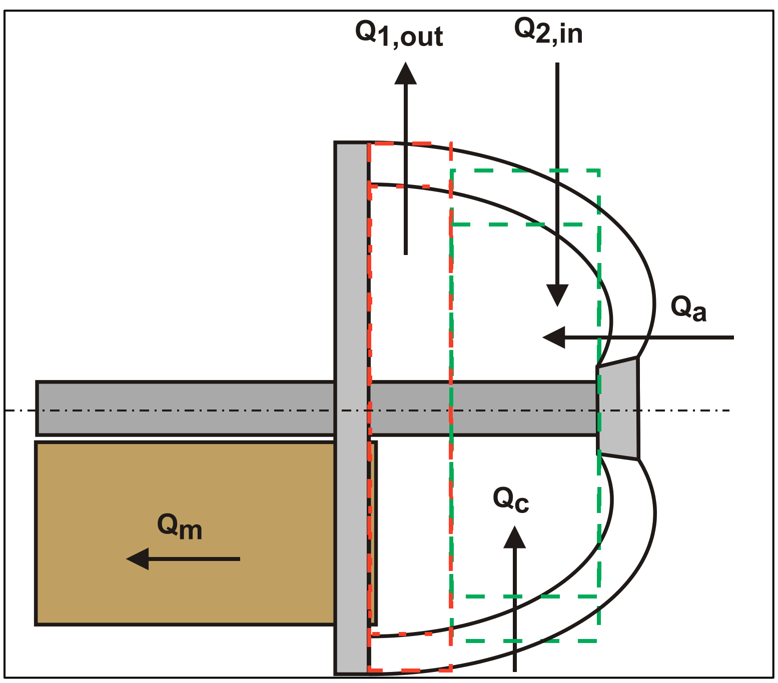

Figure 7: The flows in the cutter head.

THE VOLUME BALANCE

Figure 7 shows the different flows in and out the cutter head. The volume balance, what goes in must go out, is:

$$\begin{aligned}
&Q_{1,out} - Q_{2,in} + Q_m - Q_c - Q_a = 0\\
&\alpha_1 \cdot 2 \cdot \pi \cdot \omega \cdot r_{o,1}^2 \cdot w_1 \cdot \left(1 - P_{c,1}\right) - \left(\alpha_1 \cdot 2 \cdot \pi \cdot \omega \cdot r_{o,1}^2 - \alpha_2 \cdot 2 \cdot \pi \cdot \omega \cdot r_{o,2}^2\right) \cdot w_2 \cdot \left(1 - P_{c,2}\right)\\
&+ Q_m - Q_c - Q_a = 0
\end{aligned} \tag{13}$$

The total width (height) of the cutter head is the width of segment 1 plus the width of segment 2:

$$w = w_1 + w_2 \tag{14}$$

Equations (11), (12), (13) and (14) form a system of 4 equations with 5 unknowns α_1, α_2, ε, w_1 and w_2. Such a system requires a fifth equation or condition. Assuming α_1 and α_2 are equal because of similarity arguments 4 unknowns remain:

$$\begin{aligned}
&\left(\alpha_1 \cdot 2 \cdot \pi \cdot r_{o,1}^2 - \alpha_2 \cdot 2 \cdot \pi \cdot r_{o,2}^2\right) \cdot \left(1 - P_{c,2}\right)\\
&= \varepsilon \cdot \left(\begin{matrix} \dfrac{\rho_{m,1}}{\rho_{m,2}} \cdot \left(\left(r_{o,1}^2 - r_{i,1}^2\right) - \alpha_1 \cdot r_{o,1}^2 \cdot \left(\cot\left(\beta_{o,1}\right) - \cot\left(\beta_{i,1}\right)\right)\right) \\ -\left(\left(r_{o,2}^2 - r_{i,2}^2\right) - \alpha_2 \cdot r_{o,2}^2 \cdot \left(\cot\left(\beta_{o,2}\right) - \cot\left(\beta_{i,2}\right)\right)\right) \end{matrix} \right) \cdot \left(1 - P_{c,2}\right)
\end{aligned} \tag{15}$$

This equation can be written as:

$$\left(\alpha_1 \cdot A - \alpha_2 \cdot B\right) = \varepsilon \cdot \left(C - \alpha_1 \cdot D - E + \alpha_2 F\right)$$

$$\begin{aligned}
A &= 2 \cdot \pi \cdot r_{o,1}^2\\
B &= 2 \cdot \pi \cdot r_{o,2}^2\\
C &= \frac{\rho_{m,1}}{\rho_{m,2}} \cdot \left(r_{o,1}^2 - r_{i,1}^2\right)\\
D &= \frac{\rho_{m,1}}{\rho_{m,2}} \cdot r_{o,1}^2 \cdot \left(\cot\left(\beta_{o,1}\right) - \cot\left(\beta_{i,1}\right)\right)\\
E &= \frac{\rho_{m,2}}{\rho_{m,2}} \cdot \left(r_{o,2}^2 - r_{i,2}^2\right)\\
F &= \frac{\rho_{m,2}}{\rho_{m,2}} \cdot r_{o,2}^2 \cdot \left(\cot\left(\beta_{o,2}\right) - \cot\left(\beta_{i,2}\right)\right)
\end{aligned} \tag{16}$$

So:

$$\alpha_1 = \frac{\varepsilon \cdot \left(C - E\right) + \alpha_2 \cdot \left(B + \varepsilon \cdot F\right)}{\left(A + \varepsilon \cdot D\right)} \quad \mathit{and} \quad \alpha_2 = \frac{-\varepsilon \cdot \left(C - E\right) + \alpha_1 \cdot \left(A + \varepsilon \cdot D\right)}{\left(B + \varepsilon \cdot F\right)} \tag{17}$$

Now suppose α_1 and α_2 are equal because of similarity arguments, then:

$$\begin{gathered}\alpha_1 \cdot (A+\varepsilon \cdot D)-\alpha_1 \cdot (B+\varepsilon \cdot F)=\varepsilon \cdot (C-E) \\ \alpha=\alpha_1=\alpha_2=\frac{\varepsilon \cdot (C-E)}{(A+\varepsilon \cdot D)-(B+\varepsilon \cdot F)}\end{gathered} \tag{18}$$

The factor α does not depend on the percentages cut, only on the geometry of the cutter head. So calibrating ε on a cutterhead with a known geometry will give the correct α.

DETERMINING w_1 AND w_2

Now ε is the calibrating parameter, the two widths can be determined and from there the flows. Substituting equation (18) in equation (11) gives:

$$Q_{2,in}=\frac{\varepsilon \cdot (C-E)}{(A+\varepsilon \cdot D)-(B+\varepsilon \cdot F)} \cdot 2 \cdot \pi \cdot \omega \cdot \left(r_{o,1}^2-r_{o,2}^2\right) \cdot w_2 \cdot \left(1-P_{c,2}\right) \tag{19}$$

Substituting equation (18) in equation (8) gives:

$$Q_{1,out}=\frac{\varepsilon \cdot (C-E)}{(A+\varepsilon \cdot D)-(B+\varepsilon \cdot F)} \cdot 2 \cdot \pi \cdot \omega \cdot r_{o,1}^2 \cdot w_1 \cdot \left(1-P_{c,1}\right) \tag{20}$$

The volume balance gives now:

$$\begin{gathered}\alpha \cdot 2 \cdot \pi \cdot \omega \cdot r_{o,1}^2 \cdot \left(w-w_2\right) \cdot \left(1-P_{c,1}\right)-\alpha \cdot 2 \cdot \pi \cdot \omega \cdot \left(r_{o,1}^2-r_{o,2}^2\right) \cdot w_2 \cdot \left(1-P_{c,2}\right) \\ +Q_m-Q_c-Q_a=0\end{gathered} \tag{21}$$

This equals:

$$\begin{gathered}\alpha \cdot 2 \cdot \pi \cdot \omega \cdot r_{o,1}^2 \cdot w \cdot \left(1-P_{c,1}\right) \\ -\left(\alpha \cdot 2 \cdot \pi \cdot \omega \cdot r_{o,1}^2 \cdot \left(1-P_{c,1}\right)+\alpha \cdot 2 \cdot \pi \cdot \omega \cdot \left(r_{o,1}^2-r_{o,2}^2\right) \cdot \left(1-P_{c,2}\right)\right) \cdot w_2 \\ +Q_m-Q_c-Q_a=0\end{gathered} \tag{22}$$

So, for the width of segment 2 this gives:

$$w_2=\frac{Q_m-Q_c-Q_a+\alpha \cdot 2 \cdot \pi \cdot \omega \cdot r_{o,1}^2 \cdot w \cdot \left(1-P_{c,1}\right)}{\left(\alpha \cdot 2 \cdot \pi \cdot \omega \cdot r_{o,1}^2 \cdot \left(1-P_{c,1}\right)+\alpha \cdot 2 \cdot \pi \cdot \omega \cdot \left(r_{o,1}^2-r_{o,2}^2\right) \cdot \left(1-P_{c,2}\right)\right)} \tag{23}$$

The width of segment 1 is now:

$$w_1=w-\frac{Q_m-Q_c-Q_a+\alpha \cdot 2 \cdot \pi \cdot \omega \cdot r_{o,1}^2 \cdot w \cdot \left(1-P_{c,1}\right)}{\left(\alpha \cdot 2 \cdot \pi \cdot \omega \cdot r_{o,1}^2 \cdot \left(1-P_{c,1}\right)+\alpha \cdot 2 \cdot \pi \cdot \omega \cdot \left(r_{o,1}^2-r_{o,2}^2\right) \cdot \left(1-P_{c,2}\right)\right)} \tag{24}$$

With:

$$f=\left(\frac{\left(r_{o,1}^2-r_{o,2}^2\right)\cdot\left(1-P_{c,2}\right)}{r_{o,1}^2\cdot\left(1-P_{c,1}\right)}\right)\quad\text{and}\quad 1+f=\left(\frac{r_{o,1}^2\cdot\left(1-P_{c,1}\right)+\left(r_{o,1}^2-r_{o,2}^2\right)\cdot\left(1-P_{c,2}\right)}{r_{o,1}^2\cdot\left(1-P_{c,1}\right)}\right) \tag{25}$$

So, the width of segment 1 equals:

$$w_1=\frac{f}{(1+f)}\cdot w-\frac{1}{(1+f)}\cdot\frac{1}{2\cdot\pi\cdot\alpha\cdot\omega}\cdot\left(\frac{Q_m-Q_c-Q_a}{r_{o,1}^2\cdot\left(1-P_{c,1}\right)}\right) \tag{26}$$

The width of segment 2 can now be determined as:

$$w_2=\frac{1}{(1+f)}\cdot w+\frac{1}{(1+f)}\cdot\frac{1}{2\cdot\pi\cdot\alpha\cdot\omega}\cdot\left(\frac{Q_m-Q_c-Q_a}{r_{o,1}^2\cdot\left(1-P_{c,1}\right)}\right) \tag{27}$$

DETERMINING THE OUTFLOW AND INFLOW.

The two flows out and in of segments 1 and 2 are now:

$$\begin{gathered}Q_{1,out}=\alpha\cdot 2\cdot\pi\cdot\omega\cdot r_{o,1}^2\cdot\left(\frac{f}{(1+f)}\cdot w-\frac{1}{(1+f)}\cdot\frac{1}{2\cdot\pi\cdot\alpha\cdot\omega}\cdot\left(\frac{Q_m-Q_c-Q_a}{r_{o,1}^2\cdot\left(1-P_{c,1}\right)}\right)\right)\cdot\left(1-P_{c,1}\right)\\ Q_{2,out}=\alpha\cdot 2\cdot\pi\cdot\omega\cdot r_{o,2}^2\cdot\left(\frac{1}{(1+f)}\cdot w+\frac{1}{(1+f)}\cdot\frac{1}{2\cdot\pi\cdot\alpha\cdot\omega}\cdot\left(\frac{Q_m-Q_c-Q_a}{r_{o,1}^2\cdot\left(1-P_{c,1}\right)}\right)\right)\cdot\left(1-P_{c,2}\right)\end{gathered} \tag{28}$$

The flow into segment 2 is:

$$Q_{2,in}=2\cdot\pi\cdot\alpha\cdot\omega\cdot\left(r_{o,1}^2-r_{o,2}^2\right)\cdot\left(\frac{1}{(1+f)}\cdot w+\frac{1}{(1+f)}\cdot\frac{1}{2\cdot\pi\cdot\alpha\cdot\omega}\cdot\left(\frac{Q_m-Q_c-Q_a}{r_{o,1}^2\cdot\left(1-P_{c,1}\right)}\right)\right)\cdot\left(1-P_{c,2}\right) \tag{29}$$

SPILLAGE

The flow of soil cut into the cutter head equals the projected cross section in the direction of the swing speed and is equals to:

$$Q_c=\left(r_{o,1}\cdot\left(1-\cos\left(2\cdot\pi\cdot P_{c,1}\right)\right)\cdot w_1+r_{o,2}\cdot\left(1-\cos\left(2\cdot\pi\cdot P_{c,2}\right)\right)\cdot w_2\right)\cdot v_s \tag{30}$$

To avoid an implicit model, this can also be written in terms of an average radius $r_{c,a}$ and the full width w of the cutter head, giving:

$$Q_c=r_{c,a}\cdot\left(1-\cos\left(2\cdot\pi\cdot P_c\right)\right)\cdot w\cdot v_s \tag{31}$$

Now, with a porosity n of the soil (sand will have about 40% while for rock it depends strongly on the type of rock), the flow of solids into the cutter head is:

$$Q_s=Q_c\cdot\left(1-n\right) \tag{32}$$

The concentration of solids, assuming the concentration in the suction mouth and the concentration in the outflow of segment 1 are the same, gives:

$$C_{vs} = \frac{Q_s}{Q_m + Q_{1,out}} \tag{33}$$

The density of the outflow is:

$$\rho_m = C_{vs} \cdot \rho_q + \left(1 - C_{vs}\right) \cdot \rho_l \tag{34}$$

This is the soil flow divided by the total outflow. The spillage is now the outflow in segment 1 divided by the total outflow, giving:

$$Spillage = \frac{Q_{1,out}}{Q_m + Q_{1,out}} = \frac{Q_{1,out} \cdot C_{vs}}{Q_s} \tag{35}$$

The spillage is also the solids outflow in segment 1 divided by the total inflow of solids. In reality the concentration in the suction mouth will not be the same compared to the concentration in segment 1. The concentration in segment 1 may be larger due to gravity and mixing effects. To incorporate the gravity and mixing effect the following semi empirical equation is found for the advanced and preliminary models:

$$Spillage = \frac{Q_{1,out} \cdot \left(C_{vs} + \left(C_{vs,\max} - C_{vs} \right) \cdot \left(0.1 \cdot \left(\frac{v_t \cdot \sin\left(\theta\right) \cdot \pi \cdot r_r^2}{Q_m} \right)^2 + \left(\frac{Bu}{10.8} \right)^3 - \left(\frac{Bu}{12} \right)^4 \right) \right)}{Q_s} \tag{36}$$

$$With: \quad \mathrm{C}_{vs,\max} = \frac{Q_s}{Q_{1,out}}$$

Where the maximum concentration should be limited to a value near 50%, otherwise there is solid sand leaving segment 1, which is not physically possible. If the terminal settling velocity v_t is very small compared to the mixture velocity v_m, the gravity effect can be ignored, however for rock it plays an important role.

FILLING DEGREE

Another effect, which has not yet been considered is, is the rotating flow strong enough to bring the particles to the suction mouth? Figure 8 shows that at low revolutions the production increases with increasing revolutions. The figure suggests that below certain revolutions there is no production at all. Figure 9 shows that the cutting process takes place at the bottom of the cutter head. So, particles have to be lifted to flow to the suction mouth. This elevation depends on the ladder angle and dimensions of the cutter head. Particles will be lifted by drag forces generated by the rotating flow inside the cutter head. Now, drag forces are usually proportional to the velocity squared, in this case the circumferential velocity of the cutter head. The force that prevents the particles from being lifted is the gravitational force, resulting in a settling velocity. Based on this the ratio of the circumferential velocity of the cutter head to the terminal settling velocity, incorporating the ladder angle, squared, seems to be a good parameter to indicate the filling degree of the cutter head with particles. This gives for the FD number:

$$FillingDegree = \xi \cdot \left(\frac{\frac{D_r \cdot 2 \cdot \pi \cdot n}{2 \cdot 60} \cdot \cos\left(\theta\right)}{v_t} \right)^2 \quad and \quad FillingDegree \leq 1 \tag{37}$$

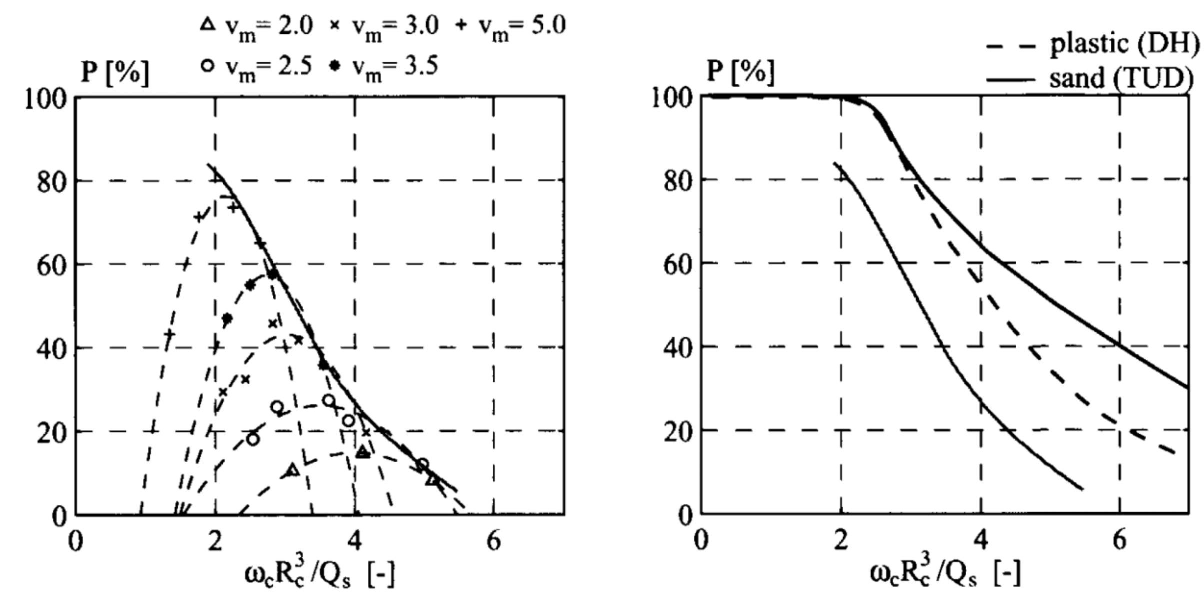

Figure 6.7: Production percentage vs. inverse of the flow number in the under-cut situation for cutting of gravel (left plot) and the results of the sand and plastic particles (right plot)

Figure 8: Production curves as a function of revolutions and mixture velocity den Burger (2003).

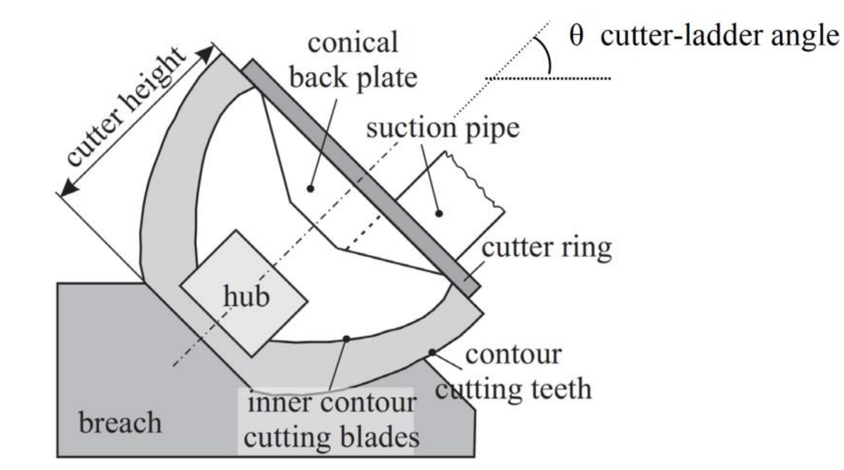

Figure 2. Model cutter positioned in breach.

Figure 9: The model cutter head in the bank.

With ξ=0.15. If the FD number is larger than 1, the filling degree equals 1, since a filling degree can never be higher that 100%. If the filling degree is, as an example, 80%, this means that 80% of the particles could reach the suction mouth. 20% of the particles never even move inside the cutter head, since they already left the cutter head immediately after cutting because of gravity. The spillage based on the flows in the cutter head of course only apply on the particles that entered the cutter head, the filling degree. The final spillage can now be determined with (spillage from equation (36)):

$$FinalSpillage = Spillage \cdot FillingDegree + \left(1 - FillingDegree\right) \qquad (38)$$

Because of the limited amount of experimental data, here a simple linear approach is used. Since in reality the cutter head revolutions are fixed, the maximum production curve or minimum spillage curve should be used as determined before. The model including the filling degree effect is named the **CHSDSG 3** model.

The filling degree is based on turbulent settling and a turbulence-based drag force, giving the squared relation of equation (37). For the Stokes region of the settling velocity, a linear relation for the filling degree is found. However, for this case the filling degree is already very high for very low revolutions, that this is not relevant. So, the filling degree approach is only relevant for large particles of rock and gravel.

To match the experiments of den Burger, the factor **ε** is about 2.45 for sand and 4.4 for rock. This can be described by:

$$\varepsilon = 2.35 + \left(4.40 - 2.35\right) \cdot \frac{v_t}{0.45} \cdot \lambda^{-0.4} \qquad (39)$$

VALIDATION

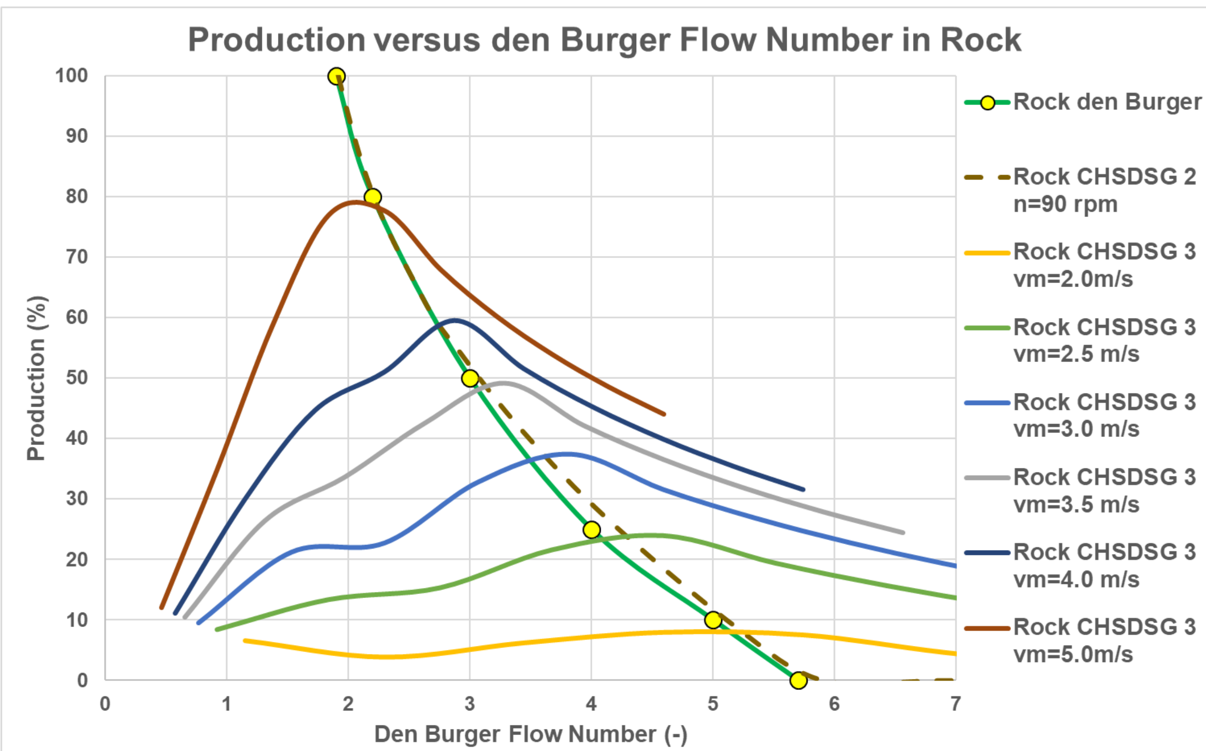

Figure 10: Production in rock n, from 20 to 200 rpm, including filling degree effect, model cutter head.

Figure 10 shows curves with this final spillage model for values of **n** from 20 rpm to 200 rpm and mixture velocities of 2 m/s to 5 m/s for the model cutter head. The curves show a real maximum at 90-100 rpm, so they do match with Figure 8 although the shape is different. The latter is not surprising, since the number of data points of den Burger (2003) was very limited.

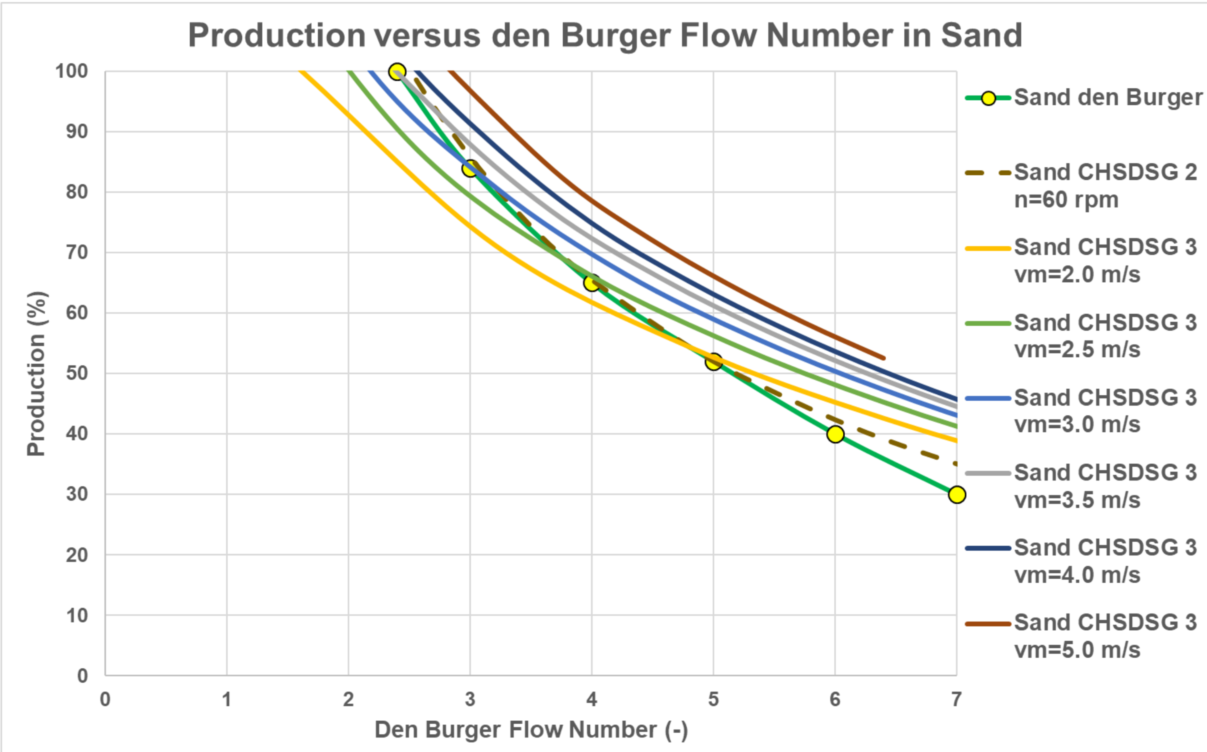

Figure 11: Production in sand, n from 20 to 200 rpm, including filling degree effect, model cutter head.

Figure 11 shows that the sand curves do not have a maximum production because of the very small settling velocity compared to rock. In fact, in sand this maximum is there but outside the range of rpm's used in the calculations.

Miltenburg (1982) carried out many experiments with 5 different cutter heads. This research was almost forgotten; however, the research was reported very detailed including the experimental data so it's like a cold case. Most of the experiments were carried out with a crown cutter head as shown in Figure 12. This cutter head has an outside diameter of 0.45 m (ring diameter 0.395 m) and a height of 0.29 m (excluding the ring). The experiments were carried out with revolutions of 100 rpm and 180 rpm and mixture velocities of 3 m/s, 4 m/s and 5 m/s. Because it was difficult to set these parameters exactly, there was some scatter in the values realized. About 50% of the cross section of the cutter head was actually cutting with swing speeds of on average 0.09 m/s, 0.18 m/s and 0.27 m/s. Also, here there was some scatter in the swing velocities. The combinations of revolutions and mixture velocities gave dimensionless Bu numbers of about 3 (n=100 rpm and v_m=5 m/s), 4 (n=100 rpm and v_m=4 m/s), 5.2 (n=100 rpm and v_m=3 m/s) and (n=180 rpm and v_m=5 m/s), 7 (n=180 rpm and v_m=4 m/s) and 9 (n=180 rpm and v_m=3 m/s). The grouping of the experimental data by Bu number is shown in Figure 15 and Figure 16. The swing speed does not influence the Bu number. The figure shows a decreasing production with an increasing Bu number, as is expected based on the theoretical model. The scatter however is very large.

Miltenburg (1982) used 6 different configurations of the crown cutter head and of course carried out the experiments overcutting and undercutting. The 6 configurations are:

1. No skirts, short cone, suction mouth at 0°, see Figure 13 for the short cone, the base case.
2. No skirts, long cone, suction mouth at 0°, see Figure 13 for the long cone.
3. No skirts, long cone, suction mouth at +30°, see Figure 13 for the long cone.
4. No skirts, long cone, suction mouth at -30°, see Figure 13 for the long cone.
5. Skirts, long cone, suction mouth at 0°, see Figure 13 for the long cone and Figure 14 for skirts.
6. Skirts, long cone, suction mouth at +30°, see Figure 13 for the long cone and Figure 14 for skirts.

Besides the 6 configurations, each test has been carried out overcutting and undercutting. So, many subsets of experiments can be made. Although Figure 15 and Figure 16 seems to show a lot of scatter, the subsets will show that often there is a reason for the variation of the spillage.

Figure 12: The crown cutter head used by Miltenburg (1982).

Figure 13: The crown cutter head (right), the short cone (left) and the long cone (right).

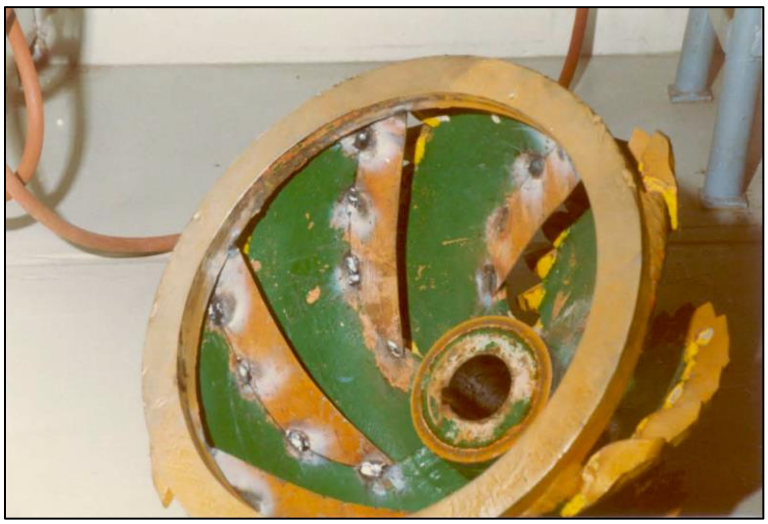

Figure 14: Skirts mounted inside the crown cutter head.

Figure 15 and Figure 16 show all data for all 6 configurations and the lower and upper production limits of the CHSDSG 2 model (so without the filling ratio effect, which is important for rock, not for sand). The lower limit is determined from n=100 rpm and v_m=3 m/s. The upper limit is determined from n=180 rpm and v_m=5 m/s. From these figures it is clear that most (about 87.5%) of the data points are in between the upper and lower limit. If data points that are more or less on the limits are not counted to be outside, 92% is within the limits (16 points outside).

CONCLUSIONS

The goal of this research, to develop an analytical model for the spillage of a cutter head, has been reached. The original idea to base this on the affinity laws of centrifugal pumps, Werkhoven et al. (2018), was successful but did not incorporate the detailed geometry of the cutter head. Using the Euler equation for centrifugal pumps gives a more detailed analytical model, not contradicting the affinity law model, since the affinity laws are a simplification of the Euler equation. The basic concept of the model is, that above a certain rpm, there is an outflow of mixture near the ring of the cutter head and in inflow of water in the rest of the cutter head, so the top part. Further there is an outflow of mixture into the suction mouth and an inflow of sand because of the cutting process. In the model also, an axial inflow of water near the hub is incorporated, but this axial flow has not really been used in the validation of the model, since it's hard to quantify. Without this axial flow the model already gives good results.

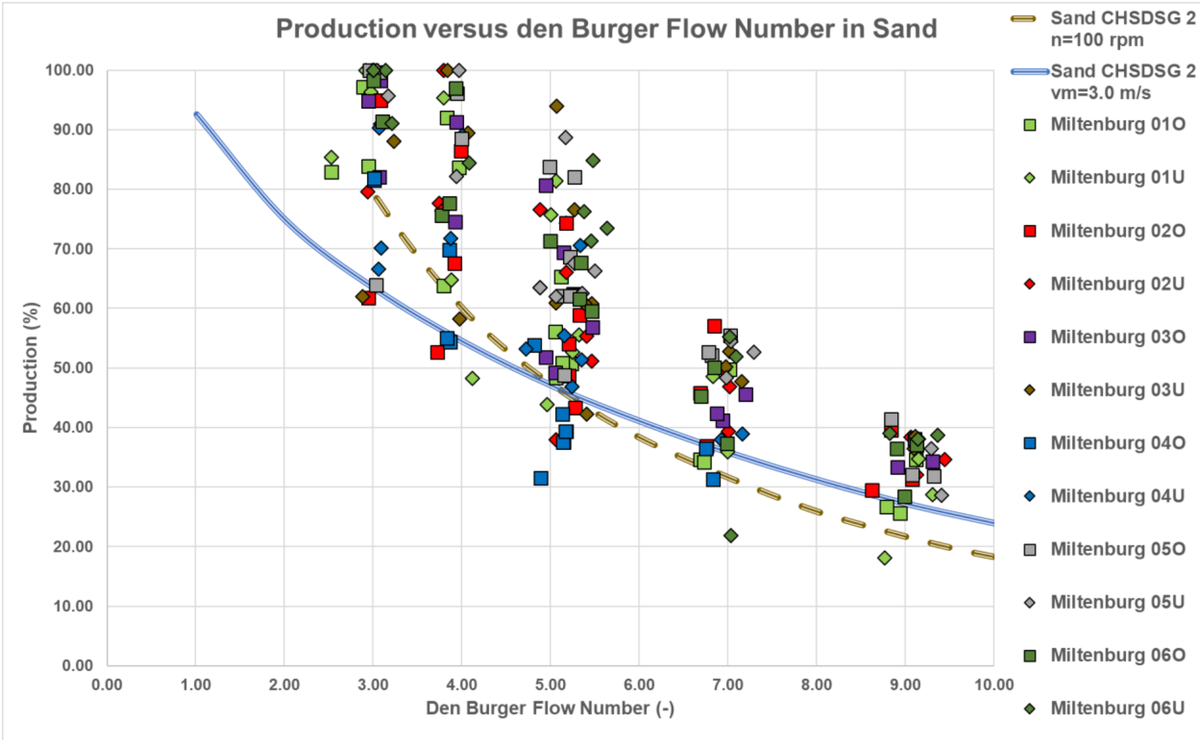

Figure 15: All experiments of Miltenburg (1982) with a rock cutter head in sand, with model lower limit.

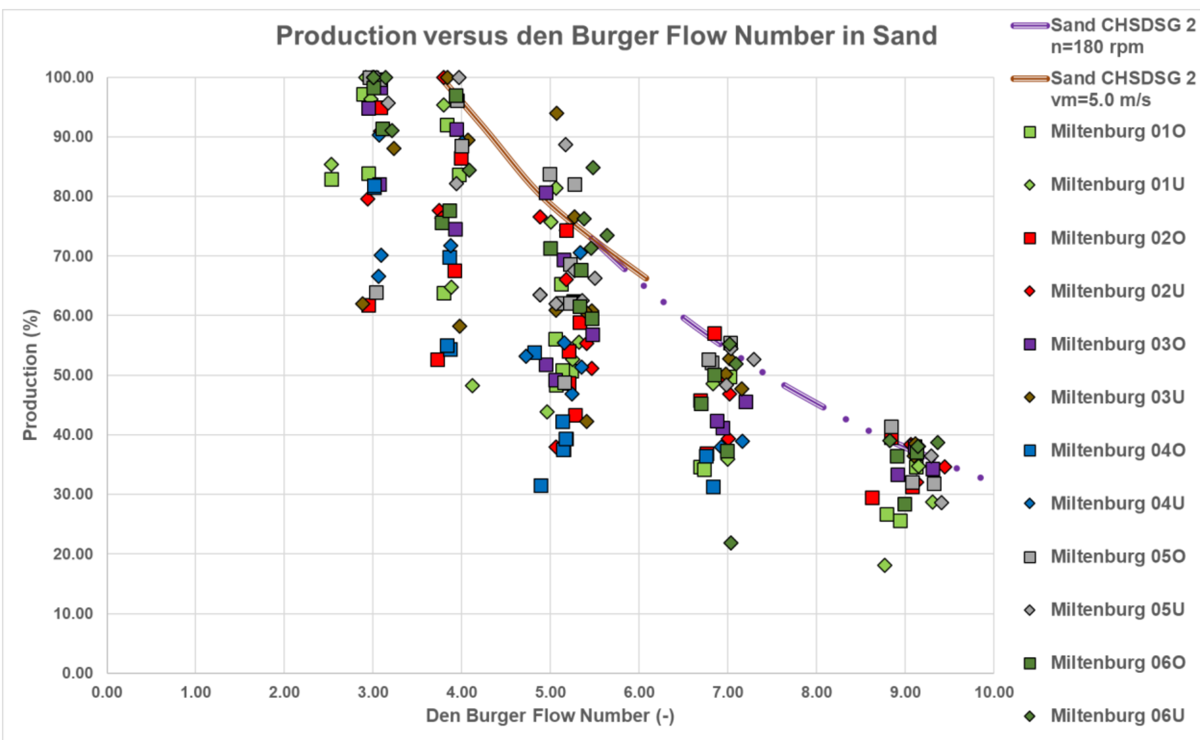

Figure 16: All experiments of Miltenburg (1982) with a rock cutter head in sand, with model upper limit.

The model is based on two continuity equations. The continuity of volume flow and the continuity of mass flow.

At first it is assumed that the mixture outflow near the ring and the mixture outflow through the suction mouth have the same solids concentration, based on the inflow of solids due to the cutting process. This assumption gives good predictions of the spillage and production at low Bu numbers, but not at high Bu numbers. At high Bu numbers (high revolutions, low mixture outflow), the spillage is underestimated in sand, but even more in rock. This is compared with the findings of Mol (1977A) and (1977B), Moret (1977A) and (1977B) and den Burger (2003). A term, increasing the concentration of the outflow near the ring is added, based on the Bu number. Of course, limiting this concentration to a reasonable maximum. This term gives a good correction for sand, but not yet for rock. So, a second term is added, based on the settling velocity of the particles in relation with the average mixture flow in the cutter head. This second term gives a good correction for gravel/rock.

The experimental data used so far is limited to Bu numbers of 6-7. When analyzing cold case data of Miltenburg (1982) Bu numbers up to 9 were found. Miltenburg carried out about 100 experiments, both overcutting and undercutting, with 6 different cutter head configurations and 5 different cutter heads. Most experiments were carried out with a crown rock cutter head, suitable for cutting rock and sand. So, these experimental data are used for the validation of the model. From these data it appeared that the original model overestimated the spillage for very large Bu numbers. The model gave almost 100% spillage, while the data showed 60%-70% spillage. An additional term has been added to the concentration of the outflow near the ring to correct for this. This additional term is based on the Bu number. With this correction a good correlation is found between the model and the experimental data.

With the final model, 92% of the data points are within the upper and lower limit of the model, based on mixture flow and revolutions. The trends based on revolutions, mixture velocity and swing speed are well predicted, although individual experiments may deviate, because of the 6 configurations.

Configurations 01, 02 and 03 show hardly any difference in the spillage. These configurations have a short cone, a long cone and a suction mouth rotated 30° in the rotation direction of the cutter head. Configuration 04 with a long cone and a 30° rotation of the suction mouth, but now counter rotated with respect to the rotation direction of the cutter head, has a spillage of up to 20% more than the base case and also with respect to configurations 02 and 03. Configurations 05 and 06 with skirts and 06 with a suction mouth rotated 30° in the rotation direction of the cutter head, both have a spillage of about 10% less than the base case and also with respect to configurations 02 and 03. So, the main measure to reduce spillage is the use of skirts, resulting in about 10% less spillage. The difference between configuration 04 on one hand and configuration 05 and 06 on the other hand already give a scatter of 30% spillage. Figure 17 and Figure 18 show the data of configurations 01, 02 and 03 with the upper and lower limits according to the model. Now only 1 data point is above the upper limit and only 2 data points are below the lower limit, regarding the production. The whole area in-between the lower and upper limit is covered by the model developed. Configurations 04, 05 and 06 require a different value for the constant $\boldsymbol{\varepsilon}$, which is set to 2.5 for the base case. Configuration 04 requires a larger value, while configurations 05 and 06 require a smaller value. The Miltenburg data do not show the filling ratio effect, most probably because only 2 cutter head revolutions were applied, and sand was used.

The den Burger number Bu should be determined using the cutter head diameter close to the ring. This diameter is often larger than the ring diameter. Since the centrifugal pump effect is determined by the actual diameter of the cutter head and not the ring diameter, the model input should also be the actual cutter diameter near the ring.

Scale laws should be applied to convert from model to prototype. These scale laws give very good results regarding the similarity of production curves, comparing model and prototype. A next publication will cover the scale laws.

All in all, the model presented here is very promising and has the advantage of easy implementation. However, to make a good prediction, the geometry of the cutter head and the operational parameters must be known. Using different cutter head geometries and particle diameters (sand, gravel or rock) may require different coefficients in the model.

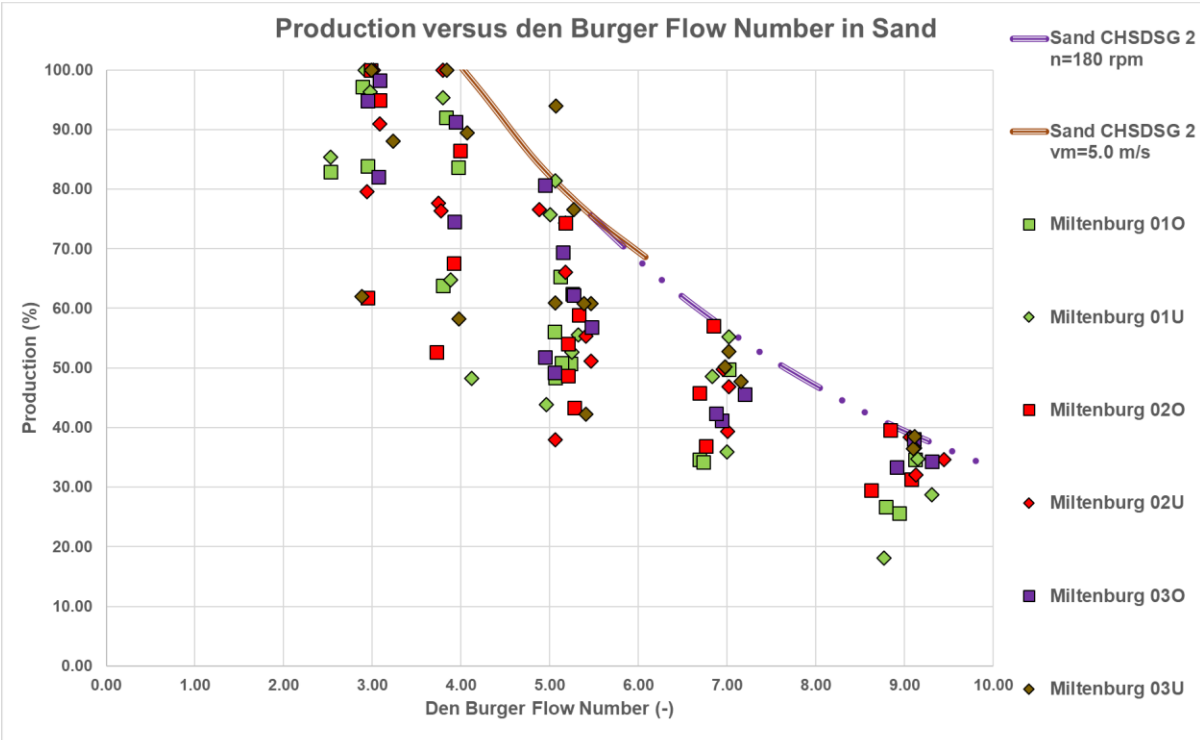

Figure 17: Experiments 1-3 of Miltenburg (1982) with a rock cutter head in sand, with model upper limit.

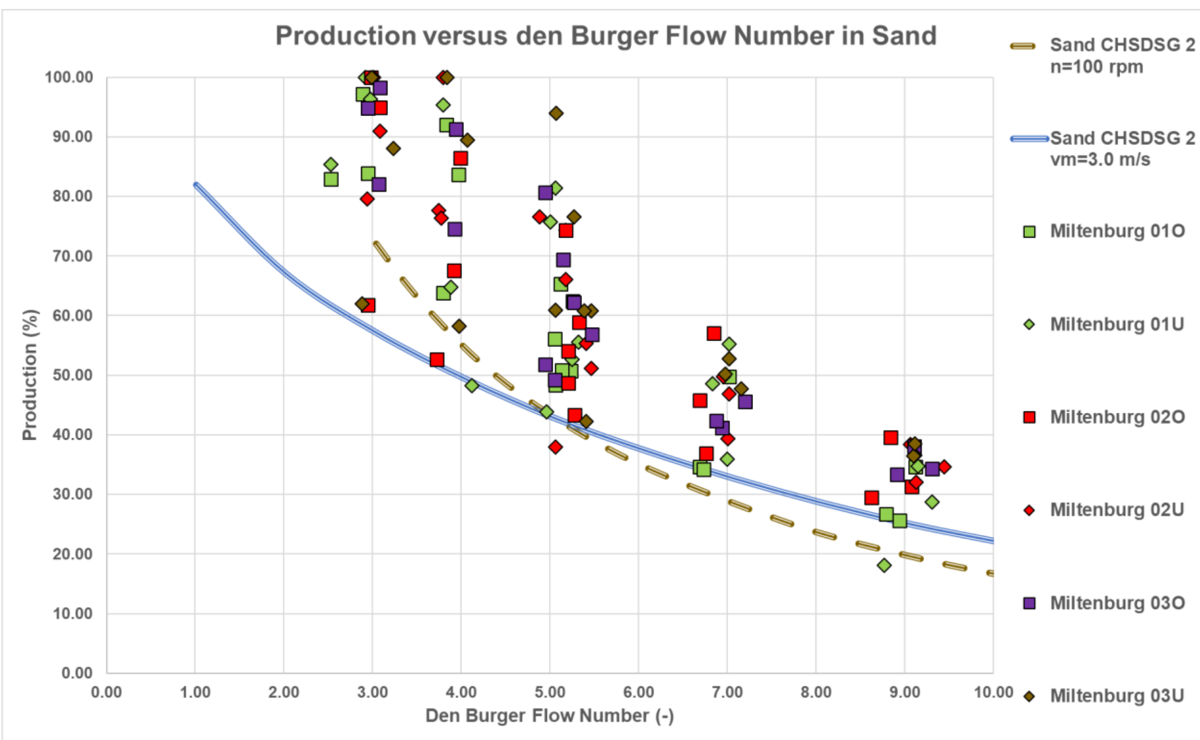

Figure 18: Experiments 1-3 of Miltenburg (1982) with a rock cutter head in sand, with model lower limit.

REFERENCES

Burger, M. (2001). Influence of ladder inclination angle and particle size on cutterhead production. *WODCON XVI.* Kuala Lumpur, Malaysia: WODA.

Burger, M. (2003). *Mixture forming processes in dredge cutter heads. PhD Thesis.* Delft, Netherlands: Delft University of Technology.

Burger, M. d., & Talmon, A. M. (2001). Mechanical transportation of particles induced by cutterblade geometry. *CEDA Dredging Days 2001.* Amsterdam, the Netherlands: CEDA.

Burger, M. d., & Talmon, A. M. (2002). Particle trajectories along a cutter blade, using the results of a CFD model for the flow. *Dredging 02 Key Technologies for Global Prosperity.* Orlando, Florida, USA: ASCE.

Burger, M. d., Vlasblom, W. J., & Talmon, A. M. (1999). Influence of operational parameters on dredge cutterhead spillage. *CEDA Dredging Days 1999.* Amsterdam, the Netherlands: CEDA.

Burger, M. d., Vlasblom, W. J., & Talmon, A. M. (2005). Design aspects for cutter heads related to the mixture forming process when cutting coarse materials. *Terra et Aqua 98*, 12-18.

Dekker, M. A., Kruyt, N. P., Burger, M. d., & Vlasblom, W. J. (2003). Experimental and numerical investigation of cutter head dredging flows. *Journal of Waterways, Port, Coastal and Ocean Engineering, Vol. (129 (5).*, 203-209.

Dekker, M. A., Vlasblom, W. J., & Kruyt, N. P. (1999). Measuring water velocities round a cutterhead. *CEDA Dredging Days 1999.* Amsterdam, the Netherlands: CEDA.

Louis, A. A. (2017). *Cutter Suction Spillage.* Delft, the Netherlands: Delft University of Technology.

Miedema, S. A. (2018). *Spillage models for a cutter head in dredging sand or gravel.* Delft, The Netherlands: Delft University of Technology.

Miltenburg, C. J. (1982). *Stroming en mengselvorming in grote snijkoppen. LaO/82/101.* Delft, the Netherlands: Delft University of Technology.

Mol, A. (1977A). *Stroombeeld rond en in cutter deel II: Vrij in water draaiend; Injecties met kleurstof. BAGT 236.* Delft, the Netherlands: Delft Hydraulics.

Mol, A. (1977B). *Stroombeeld rond en in cutter deel III: Stroombeeld in cutter bij kunstmatige taluds; Injecties met stukjes plastic. BAGT 237.* Delft, the Netherlands: Delft Hydraulics.

Moret, G. E. (1977A). *Stroombeeld rond en in cutter deel I: Stroombeeld rondom cutter bij kunstmatige taluds.* Delft, the Netherlands: Delft Hydraulics, BAGT 235.

Moret, G. E. (1977B). *Stroombeeld rond en in cutter deel IV: Stroombeeld bij kunstmatige taluds.* Delft, the Netherlands: Delft Hydraulics, BAGT 238.

Steinbusch, P. J., Vlasblom, W. J., & Burger, M. d. (1999). Numerical simulation of the flow generated by cutter heads. *Hydrotransport 14* (pp. 435-443). Cranfield, UK: BHRG.

Talmon, A. M., Vlasblom, W. J., & Burger, M. d. (2010). Cutter production and kinematics of mixture forming. *WODCON XIX* (pp. 838-847). Beijing, China: WODA.

Vlasblom, W. J., & Talmon, A. M. (2006). Spillage problem of cutter suction dredgers. *2nd Chinese International Dredging Congress.* Guangzhou, China: CHIDA.

Werkhoven, J. J., Nieuwboer, B. J., Louis, A. A., Ramsdell, R. C., & Miedema, S. A. (2018). A pseudo analytical model for CSD spillage due to rotational velocity induced flow. *Dredging Summit & Expo 18* (p. 18). Norfolk, Virginia, USA: WEDA.

Werkhoven, J. J., Nieuwboer, B. J., Louis, A. A., Ramsdell, R. C., & Miedema, S. A. (2019A). A pseudo analytical model for CSD spillage due to rotational velocoty induced flow. *Terra et Aqua 153*, 15.

Werkhoven, J. J., Nieuwboer, B. J., Ramsdell, R. C., & Miedema, S. A. (2019B). CSD Spillage Model for Sand and Rock. *World Dredging Conference* (p. 17). Shanghai, China: CHIDA, EADA, WODA.

CITATION

Miedema, Sape A. “Cutter Head Spillage when Dredging Sand or Gravel,” *Proceedings of the Western Dredging Association Dredging Summit & Expo ‘19, Chicago, IL, USA*, June 4-7, 2019.

NOMENCLATURE

Bu	Den Burger dimensionless number	**-**
$\mathbf{C_{vs}}$	Spatial volumetric concentration	**-**
$\mathbf{D_{p,s}}$	Pipe diameter suction pipe	**m**
$\mathbf{D_r}$	Cutter ring diameter	**m**
f	Radii factor	**-**
FR	Filling ratio dimensionless number	**-**
n	Porosity	**-**
$\mathbf{\Delta p}$	Pressure difference	**kPa**
$\mathbf{\Delta p_E}$	Euler pressure difference	**kPa**
$\mathbf{\Delta p_{E,1}}$	Euler pressure difference segment 1	**kPa**
$\mathbf{\Delta p_{E,2}}$	Euler pressure difference segment 2	**kPa**
$\mathbf{\Delta p_1}$	Pressure difference segment 1	**kPa**
$\mathbf{\Delta p_2}$	Pressure difference segment 2	**kPa**
$\mathbf{P_c}$	Percentage circumference involved in cutting (as a factor)	**-**
$\mathbf{P_{c,1}}$	Percentage circumference involved in cutting (as a factor) segment 1	**-**
$\mathbf{P_{c,2}}$	Percentage circumference involved in cutting (as a factor) segment 2	**-**
q	Specific flow (per meter width)	$\mathbf{m^2/s}$
$\mathbf{q_{1,out}}$	Specific outflow segment 1	$\mathbf{m^2/s}$
$\mathbf{q_{2,out}}$	Specific outflow segment 2	$\mathbf{m^2/s}$
$\mathbf{q_{2,in}}$	Specific inflow segment 2	$\mathbf{m^2/s}$
Q	Flow	$\mathbf{m^3/s}$
$\mathbf{Q_a}$	Axial flow	$\mathbf{m^3/s}$
$\mathbf{Q_c}$	Cut production situ soil	$\mathbf{m^3/s}$
$\mathbf{Q_s}$	Cut production solids	$\mathbf{m^3/s}$
$\mathbf{Q_m}$	Mixture flow suction mouth	$\mathbf{m^3/s}$
$\mathbf{Q_{1,out}}$	Mixture outflow segment 1	$\mathbf{m^3/s}$
$\mathbf{Q_{2,out}}$	Mixture outflow segment 2	$\mathbf{m^3/s}$
$\mathbf{Q_{2,in}}$	Mixture inflow segment 2	$\mathbf{m^3/s}$
$\mathbf{r_o}$	Outer radius	**m**
$\mathbf{r_i}$	Inner radius	**m**
$\mathbf{r_{o,1}}$	Outer radius segment 1	**m**
$\mathbf{r_{i,1}}$	Inner radius segment 1	**m**
$\mathbf{r_{o,2}}$	Outer radius segment 2	**m**
$\mathbf{r_{i,2}}$	Inner radius segment 2	**m**
$\mathbf{r_{c,a}}$	Average outer cutter radius	**m**
$\mathbf{r_r}$	Cutter ring radius	**m**
$\mathbf{u_o}$	Circumferential velocity outer radius	**m/s**
$\mathbf{u_i}$	Circumferential velocity inner radius	**m/s**
$\mathbf{v_s}$	Swing speed	**m/s**
$\mathbf{v_m}$	Mixture velocity suction pipe	**m/s**
$\mathbf{v_t}$	Terminal settling velocity particles	**m/s**

w	Width (or height) of cutter head	**m**
w_1	Width segment 1	**m**
w_2	Width segment 2	**m**
α	Flow factor	**-**
α_1	Flow factor segment 1	**-**
α_2	Flow factor segment 2	**-**
β_o	Blade angle outer radius	**rad**
$\beta_{o,1}$	Blade angle outer radius segment 1	**rad**
$\beta_{o,2}$	Blade angle outer radius segment 2	**rad**
β_i	Blade angle inner radius	**rad**
$\beta_{i,1}$	Blade angle inner radius segment 1	**rad**
$\beta_{i,2}$	Blade angle inner radius segment 2	**rad**
ε	Factor pressure	**-**
ρ_l	Density carrier liquid (water)	**ton/m^3**
ρ_q	Density solids (quarts)	**ton/m^3**
ρ_m	Mixture density	**ton/m^3**
$\rho_{m,1}$	Mixture density segment 1	**ton/m^3**
$\rho_{m,2}$	Mixture density segment 2	**ton/m^3**
ω	Radial frequency cutter head	**rad/s**
ξ	Factor in FD (filling degree) dimensionless number	**-**
θ	Ladder angle	**rad**

